# The Voronoi diagram of three lines in $\mathbb{R}^3$

Hazel Everett[†] Daniel Lazard[‡] Sylvain Lazard[†] Mohab Safey El Din[‡]

**Abstract**

We give a complete description of the Voronoi diagram of three lines in $\mathbb{R}^3$. In particular, we show that the topology of the Voronoi diagram is invariant for three lines in general position, that is, that are pairwise skew and not all parallel to a common plane. The trisector consists of four unbounded branches of either a non-singular quartic or of a cubic and line that do not intersect in real space. Each cell of dimension two consists of two connected components on a hyperbolic paraboloid that are bounded, respectively, by three and one of the branches of the trisector. The proof technique, which relies heavily upon modern tools of computer algebra, is of interest in its own right.

This characterization yields some fundamental properties of the Voronoi diagram of three lines. In particular, we present linear semi-algebraic tests for separating the two connected components of each two-dimensional Voronoi cell and for separating the four connected components of the trisector. We also show that the arcs of the trisector are monotonic in some direction. These properties imply that points on the trisector of three lines can be sorted along each branch using only linear semi-algebraic tests.

[†]LORIA - INRIA Lorraine - University Nancy 2, Firstname.Name@loria.fr

[‡]LIP6 - INRIA Rocquencourt - University Pierre et Marie Curie, Firstname.Name@lip6.fr

# 1 Introduction

The Voronoi diagram of a set of disjoint objects is a decomposition of space into cells, one cell per object, such that the cell associated with an object consists of all points that are closer to that object than to any other object. In this paper, we consider the Voronoi diagram of lines in $\mathbb{R}^3$ under the Euclidean metric.

Voronoi diagrams have been the subject of a tremendous amount of research. For points, these diagrams, their complexity and optimal algorithms are well understood and robust efficient implementations exist for computing them in any dimension (see for instance [1, 2, 4, 5, 6, 7, 14, 25, 34]) even though some important problems remain and are addressed in recent papers. The same is true for segments and polygons in two dimensions [17].

For lines, segments, and polyhedra in three dimensions much less is known. In particular, determining the combinatorial complexity of the Voronoi diagram of $n$ lines or line segments in $\mathbb{R}^3$ is an outstanding open problem. The best known lower bound is $\Omega(n^2)$ and the best upper bound is $O(n^{3+\varepsilon})$ [35]. It is conjectured that the complexity of such diagrams is near-quadratic. In the restricted case of a set of $n$ lines with a fixed number, $c$, of possible orientations, Koltun and Sharir have shown an upper bound of $O(n^{2+\varepsilon})$, for any $\varepsilon > 0$ [19].

There are few algorithms for computing exactly the Voronoi diagram of linear objects. Most of this work has been done in the context of computing the medial axis of a polyhedron, *i.e.,* the Voronoi diagram of the faces of the polyhedron [9, 23]. Recently, some progress has been made on the related problem of computing arrangements of quadrics (each cell of the Voronoi diagram is a cell of such an arrangement) [3, 18, 24, 31, 32]. Finally, there have been many papers reporting algorithms for computing approximations of the Voronoi diagram (see for instance [10, 13, 16, 36]).

In this paper, we address the fundamental problem of understanding the structure of the Voronoi diagram of three lines. A robust and effective implementation of Voronoi diagrams of three-dimensional linear objects requires a complete and thorough treatment of the base cases, that is the diagrams of three and four lines, points or planes. We also strongly believe that this is required in order to make progress on complexity issues, and in particular for proving tight worst-case bounds. We provide here a full and complete characterization of the geometry and topology of the elementary though difficult case of the Voronoi diagram of three lines in general position.

**Main results.** Our main result, which settles a conjecture of Koltun and Sharir [19], is the following (see Figure 1).

**Theorem 1** *The topology of the Voronoi diagram of three pairwise skew lines that are not all parallel to a common plane is invariant. The trisector consists of four infinite branches of either a non-singular quartic*[1] *or of a cubic and line that do not intersect in* $\mathbb{P}^3(\mathbb{R})$. *Each cell of dimension two consists of two connected components on a hyperbolic paraboloid that are bounded, respectively, by three and one of the branches of the trisector.*

The proof technique, which relies heavily upon modern tools of computer algebra, is of interest in its own right.

This characterization yields some fundamental properties of the Voronoi diagram of three lines which are likely to be critical for the analysis of the complexity and the development of efficient algorithms for computing Voronoi diagrams and medial axis of lines or polyhedra. In particular, we obtain the following.

**Theorem 2** *Each of the branches of the trisector of three pairwise skew lines that are not all parallel to a common plane is monotonic in some direction. Furthermore, there is a linear semi-algebraic test for*

*(i) deciding on which of the two connected components of a two-dimensional cell a point lies,*
*(ii) deciding on which of the four branches of the trisector a point lies,*
*(iii) ordering points on each branch of the trisector.*

[1] By non-singular quartic, we mean an irreducible curve of degree four with no singular point in $\mathbb{P}^3(\mathbb{C})$.

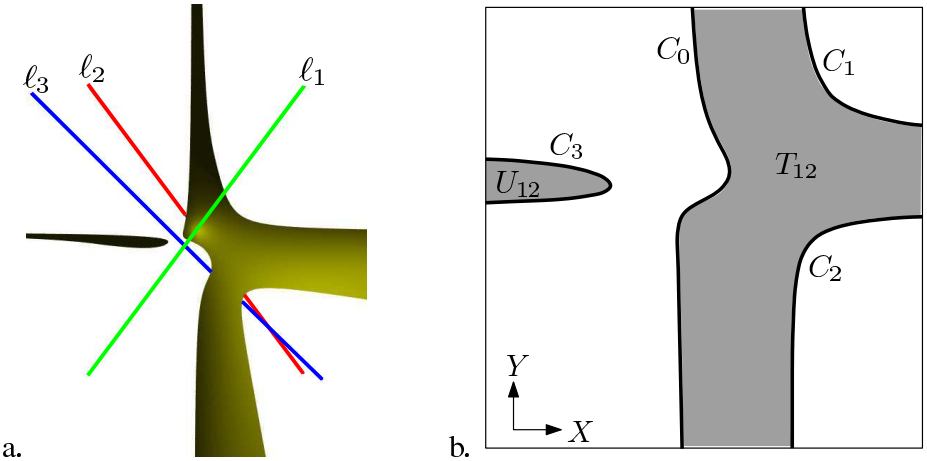


Figure 1: Voronoi diagram of 3 lines $\ell_1$, $\ell_2$, and $\ell_3$ in general position: (a) Voronoi 2D face of $\ell_1$ and $\ell_2$, *i.e.,* set of points equidistant to $\ell_1$ and $\ell_2$ and closer to them than to $\ell_3$. (b) Orthogonal projection of a 2D face on a plane $\mathcal{P}$ with coordinate system $(X,Y)$ such that the plane's normal is parallel to the common perpendicular of $\ell_1$ and $\ell_2$ and such that the $X$ and $Y$-axis are parallel to the two bisector lines (in $\mathcal{P}$) of the projection of $\ell_1$ and $\ell_2$ on $\mathcal{P}$; the face is bounded by four branches of a non-singular quartic.

The rest of the paper is organized as follows. The next section gives the proof of Theorem 1. In Section 3, we present some fundamental properties of the Voronoi diagram of three lines and prove Theorem 2. Finally, we give, in Section 4, a geometric characterization of the configurations of three lines in general position such that their trisector contains a line.

## 2 Proof of Theorem 1

We consider three lines in *general position*, that is, that are pairwise skew and not all parallel to the same plane. The idea is to prove that the topology of the trisector is invariant by continuous deformation on the set of all triplets of three lines in general position and that this set is connected. The result then follows from the analysis of any example.

We show that the trisector is always homeomorphic to four lines that do not pairwise intersect. To prove this, we show that the trisector is always non-singular in $\mathbb{P}^3(\mathbb{R})$ and has four simple real points at infinity. To show that the trisector is always non-singular, we study the type of the intersection of two bisectors, which are hyperbolic paraboloids.

We use the classic result that the intersection of two quadrics is a non-singular quartic (in $\mathbb{P}^3(\mathbb{C})$) unless the characteristic equation of their pencil has (at least) a multiple root. In order to determine when this equation has a multiple root, we determine when its discriminant $\Delta$ is zero.

This discriminant has several factors, some of which are trivially always positive. The remaining, so-called "*gros facteur*", can be shown, using Safey's software [26], to be never negative. This implies that it is zero only when all its partial derivatives are zero. We thus consider the system that consists of the *gros facteur* and all its partial derivatives, and compute its Gröbner basis. This gives three equations of degree six. We consider separately two components of solutions, one for which a (simple) polynomial $F$ is zero, the other for which $F \neq 0$.

When $F \neq 0$, some manipulations and simplifications, which are interesting in their own rights, yield another Gröbner basis, with the same real roots, which consists of three equations of degree four. We show that one of these equations has no real root which implies that the system has no real root and thus that $\Delta = 0$ has no real root on the considered component. We can thus conclude that, in this case, the trisector is always a

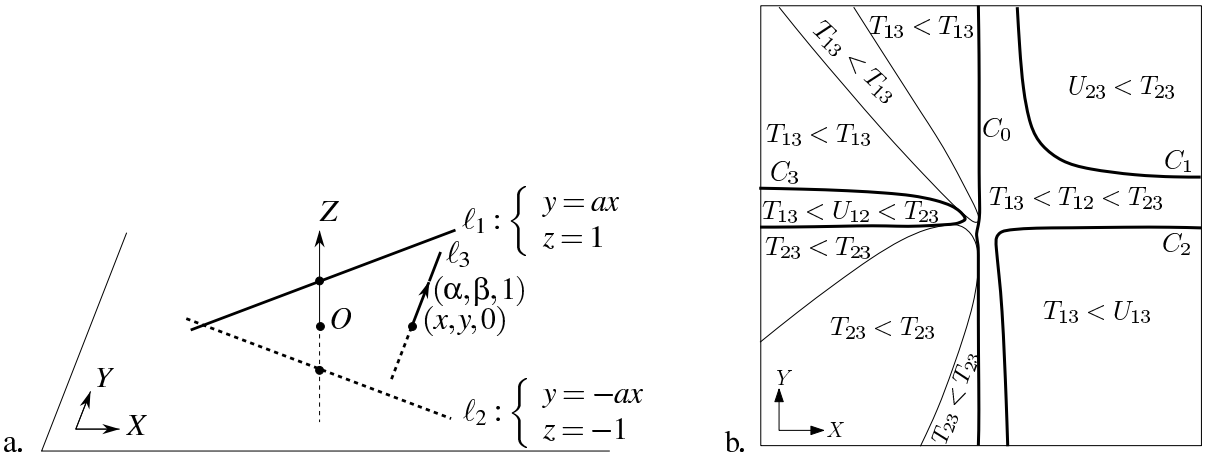


Figure 2: (a) 3 lines in general position. (b) Ordering of the connected components of the cells of the Voronoi diagram above each region induced by the projection of the trisector and silhouette curves of the bisectors; $U_{ij}$ and $T_{ij}$ denote the connected components of the cell $V_{ij}$ that are bounded by one and three arcs of the trisector, respectively; the ordering over the small cell in the middle is $T_{13} < T_{13} < T_{23} < T_{23}$.

non-singular quartic in $\mathbb{P}^3(\mathbb{R})$. When $F = 0$, we show, by substituting $F = 0$ in $\Delta$ and by using the classification of the intersection of quadrics over the reals [12], that the trisector is a cubic and a line that do not intersect in $\mathbb{P}^3(\mathbb{R})$.

We can thus conclude that the trisector is always a non-singular quartic or a cubic and a line that do not intersect in real space and thus that the trisector is always non-singular in $\mathbb{P}^3(\mathbb{R})$.

In the rest of this section, we prove Theorem 1.

## 2.1 Preliminaries

Let $\ell_1$, $\ell_2$, and $\ell_3$ be three lines in general position, *i.e.,* that are pairwise skew and not all parallel to a common plane. Refer to Figure 2(a). Let $(X,Y,Z)$ denote a Cartesian coordinate system. Without loss of generality, we assume that $\ell_1$ and $\ell_2$ are both horizontal, pass through $(0,0,1)$ and $(0,0,-1)$ respectively, and have directions that are symmetric with respect to the $XZ$-plane. More precisely, we assume that line $\ell_1$ is defined by point $p_1 = (0,0,1)$ and vector $v_1 = (1,a,0)$, and line $\ell_2$ by point $p_2 = (0,0,-1)$ and vector $v_2 = (1,-a,0)$, $a \in \mathbb{R}$. Moreover, since the three lines are not all parallel to a common plane, $\ell_3$ is not parallel to the plane $z = 0$, and so we can assume that line $\ell_3$ is defined by point $p_3 = (x,y,0)$ and vector $v_3 = (\alpha,\beta,1)$, $x,y,\alpha,\beta \in \mathbb{R}$.

We denote by $\mathcal{H}_{i,j}$ the bisector of lines $\ell_i$ and $\ell_j$ and by $V_{ij}$ the Voronoi cell of lines $\ell_i$ and $\ell_j$, *i.e.,* the set of points equidistant to $\ell_i$ and $\ell_j$ and closer to them than to $\ell_k$, $k \neq i,j$. We recall the following well-known elementary facts. The bisector of two pairwise skew lines is a right hyperbolic paraboloid, that is, has equation of the form $Z = \gamma XY$, $\gamma \in \mathbb{R}$, in some coordinate system (see for instance[19]). The Voronoi cells are connected and star-shaped [21].

## 2.2 Algebraic structure of the trisector, Part I

The trisector of our three lines is the intersection of two right hyperbolic paraboloids, say $\mathcal{H}_{1,2}$ and $\mathcal{H}_{1,3}$. The intersection of two arbitrary hyperbolic paraboloids may be singular; it may be a nodal or cuspidal quartic, two secant conics, a cubic and a line that intersect, a conic and two lines crossing on the conic, etc (see [12, Table 4]). We show here that the trisector is always non-singular by studying the characteristic polynomial of the pencil of $\mathcal{H}_{1,2}$ and $\mathcal{H}_{1,3}$.

Let $Q_{1,2}$ and $Q_{1,3}$ be matrix representations of $\mathcal{H}_{1,2}$ and $\mathcal{H}_{1,3}$, *i.e.* the Hessian of the quadratic form associated with the surface (see, for instance, [11]). The *pencil* of $Q_{1,2}$ and $Q_{1,3}$ is the set of linear combinations

of them, that is, $P(\lambda) = \{\lambda Q_{1,2} + Q_{1,3},\ \forall \lambda \in \bar{\mathbb{R}}\}$. The *characteristic polynomial* of the pencil is the determinant, $\mathcal{D}(\lambda) = \det(P(\lambda))$, which is a degree four polynomial in $\lambda$. The intersection of any two quadrics is a non-singular quartic, in $\mathbb{P}^3(\mathbb{C})$, if and only if the characteristic equation of the corresponding pencil does not have any multiple roots (in $\mathbb{C}$) [33] (see also [12]). A non-singular quartic of $\mathbb{P}^3(\mathbb{C})$ is, in $\mathbb{P}^3(\mathbb{R})$, either empty or a non-singular quartic. Thus, since the trisector of our three lines cannot be the empty set in $\mathbb{R}^3$, the trisector is a smooth quartic in $\mathbb{P}^3(\mathbb{R})$ if and only if the characteristic equation of the pencil does not have any multiple roots (in $\mathbb{C}$).

The characteristic polynomial of the pencil is fairly complicated (roughly one page in the format of Eq. (1)). However, by a change of variable $\lambda \rightarrow 2\lambda(1+\alpha^2+\beta^2)$ and by dividing out the positive factor $(1+a^2)^2(1+\alpha^2+\beta^2)^3$, the polynomial simplifies, without changing its roots, to the following, which we still denote by $\mathcal{D}(\lambda)$ for simplicity.

$$\begin{aligned}\mathcal{D}(\lambda) = {} & (\alpha^2+\beta^2+1)\,a^2\lambda^4 - 2a\,(2a\beta^2 + ay\beta + a\alpha x - \beta\alpha + 2a + 2a\alpha^2 - \beta\alpha a^2)\,\lambda^3 \\ & + (\beta^2 + 6a^2\beta^2 - 2\beta x a^3 - 6\beta\alpha a^3 + 6y\beta a^2 - 6a\beta\alpha - 2a\beta x + 6\alpha x a^2 + y^2a^2 - 2a\alpha y + x^2a^2 - 2y\alpha a^3 + 6a^2\alpha^2 + a^4\alpha^2 + 4a^2)\,\lambda^2 \\ & - 2\,(xa - ya^2 - 2\beta a^2 - \beta + 2a\alpha + \alpha a^3)\,(xa - y - \beta + a\alpha)\,\lambda + (1+a^2)\,(xa - y - \beta + a\alpha)^2 \qquad (1)\end{aligned}$$

In the sequel, all polynomials are considered over the reals, that is for $\lambda, a, \alpha, \beta, x, y$ in $\mathbb{R}$, unless specified otherwise. We start by studying the sign of $\mathcal{D}(\lambda)$.

**Lemma 3** *The characteristic polynomial $\mathcal{D}(\lambda)$ is never negative.*

**Proof.** We prove that the real semi-algebraic set $\mathcal{S} = \{\chi = (\lambda, a, x, y, \alpha, \beta) \in \mathbb{R}^6 \mid \mathcal{D}(\chi) < 0\}$ is empty using a development version of the RAGLIB Maple library [26] which is based on the algorithm presented in [28]. The algorithm computes at least one point per connected component of such a semi-algebraic set and we observe that, in our case, this set is empty. Before presenting our computation, we first describe the general idea of this algorithm.

Suppose first that $\mathcal{S} \neq \mathbb{R}^6$ and let $\mathcal{C}$ denote any connected component of $\mathcal{S}$. We consider here $\mathcal{D}$ as a function of all its variables $\chi = (\lambda, a, x, y, \alpha, \beta) \in \mathbb{R}^6$. The algorithm first computes the set of generalized critical values[2] of $\mathcal{D}$ (see [28] for an algorithm computing them). The image by $\mathcal{D}$ of $\mathcal{C}$ is an interval whose endpoints[3] are zero and either a negative generalized critical value or minus infinity. For any $v$ in this interval, there is a point $\chi_0 \in \mathcal{C}$ such that $\mathcal{D}(\chi_0) = v$, and the connected component containing $\chi_0$ of the hypersurface $\mathcal{D}(\chi) = v$ is included in the connected component $\mathcal{C}$. Hence, a point in $\mathcal{C}$ can be found by computing a point in each connected component of $\mathcal{D}(\chi) = v$. It follows that we can compute at least a point in every connected component of the semi-algebraic set $\mathcal{S}$ defined by $\mathcal{D}(\chi) < 0$ by computing at least one point in every connected component of the real hypersurface defined by $\mathcal{D}(\chi) = v$ where $v$ is any value smaller than zero and larger than the largest negative generalized critical value, if any. Finally, a randomly chosen point $p$ in $\mathbb{R}^6$ also needs to be added, if $\mathcal{D}(p) < 0$, to ensure that we find a point in every connected component of $\mathcal{S}$ in the case where $\mathcal{S} = \mathbb{R}^6$.

Now, computing at least one point in every connected component of a hypersurface defined by $\mathcal{D}(\chi) = v$ can be done by computing the critical points of the distance function between the surface and a point, say the origin,

[2]Recall that the (real) critical values of $\mathcal{D}$ are the values of $\mathcal{D}$ at its critical points $\chi$, i.e., the points $\chi$ at which the gradient of $\mathcal{D}$ is zero. The asymptotic critical values are similarly defined as, roughly speaking, the values taken by $\mathcal{D}$ at critical points at infinity, that is, the values $c \in \mathbb{R}$ such that the hyperplane $z = c$ is tangent to the surface $z = \mathcal{D}(\chi)$ at infinity (this definition however only holds for two variables, *i.e.*, $\chi \in \mathbb{R}^2$). More formally, the asymptotic critical values were introduced by Kurdyka et al. [20] as the limits of $\mathcal{D}(\chi_k)$ where $(\chi_k)_{k\in\mathbb{N}}$ is a sequence of points that goes to infinity while $\|\chi_k\| \cdot \|\mathbf{grad}_{\chi_k} \mathcal{D}(\chi_k)\|$ tends to zero. The generalized critical values are the critical values and asymptotic critical values. *The set of generalized critical values contains all the extrema of function $\mathcal{D}$, even those that are reached at infinity.*

[3]Since $\mathcal{S} \neq \mathbb{R}^6$, the boundary of $\mathcal{C}$ is not empty and consists of points $\chi$ such that $\mathcal{D}(\chi) = 0$. The image of the connected set $\mathcal{C}$ by the continuous function $\mathcal{D}$ is an interval. Hence, zero is an endpoint of the interval $\mathcal{D}(\mathcal{C})$. The other endpoint is either an extremum of $\mathcal{D}$ (and thus a generalized critical value) or minus infinity.

that is, by solving the system $\mathcal{D}(\chi) = v$, $\chi \times \mathrm{grad}(\mathcal{D})(\chi) = 0$. This conceptually simple approach, developed in [27], is, however, not computationally efficient. The efficient algorithm presented in [28] computes instead critical points of projections, combining efficiently the strategies given in [30] and [29].

Table 1 (in Appendix F) shows the result of the computation of at least one point in every connected component of $\mathcal{S}$.[4] We observe that this set is empty, implying that $\mathcal{D}(\chi) \geqslant 0$ for all $\chi \in \mathbb{R}^6$. It should be noted that these computations are very fast: they take roughly 3 seconds of elapsed time on a standard PC. □

Let $\Delta$ be the discriminant of the characteristic polynomial $\mathcal{D}(\lambda)$ (with respect to $\lambda$). Recall that $\mathcal{D}(\lambda)$ admits a multiple root if and only if its discriminant is zero.

**Corollary 4** *The discriminant $\Delta$ is never negative.*

**Proof.** By Lemma 3, $\mathcal{D}(\lambda)$ is either always positive or has a multiple root. If a degree-four polynomial is always positive, then it easily follows from the definition that its discriminant is positive [8, §3 p. 119]. Furthermore, if a polynomial has a multiple root then its discriminant is zero. □

**Remark.** *The proof that $\Delta$ is never negative can also be proved with the* RAGLIB *library, as in the proof of Lemma 3, but the computation is then a lot more time consuming (roughly 10 hours instead of 3 seconds).*

The discriminant $\Delta$ of the characteristic polynomial, computed with Maple [22], is equal to

$$16a^4\,(ax-y-\beta+a\alpha)^2\,(y+ax-a\alpha-\beta)^2 \tag{2}$$

times a factor that we refer to as the *gros facteur* which is a rather large polynomial of which we only show 2 out of 22 lines:

$$\begin{aligned}\text{gros_facteur} = {} & 8a^8\alpha^4y^2+7a^4\beta^2x^4-4a\beta^3x+16a^8\beta^4x^4+32a^4\alpha^2y^2+2a^6\alpha^2\beta^4x^2+38a^8\alpha^2x^2+2y^4\beta^2a^4\alpha^2+44a^8\alpha^2\beta^2x^2\\ & \cdots+22a^4y^2\beta^2x^2+y^6a^6+\alpha^2y^6a^6-2\beta x\alpha y^5a^6+x^6a^6+10\beta x^3a^7\alpha^2+2y\alpha^3a^7x^2-32a^3\alpha^2y^2\beta x+28a^3\beta^2x^2\alpha y-24a^2\beta^3y\alpha x.\end{aligned} \tag{3}$$

**Lemma 5** *The discriminant $\Delta$ is equal to zero if and only if the* gros facteur *and all its partial derivatives are equal to zero.*

**Proof.** The polynomial (2) is not equal to zero under our general position assumption. Indeed, $a = 0$ is equivalent to saying that lines $\ell_1$ and $\ell_2$ are parallel and the two other factors of (2) are equal to the square of $\det(p_i - p_3, v_i, v_3)$, for $i = 1,2$, and thus are equal to zero if and only if $\ell_i$ and $\ell_3$ are coplanar, for $i = 1,2$. It follows that (2) is always strictly positive. Thus, the discriminant $\Delta$ is equal to zero if and only if the *gros facteur* is zero. Furthermore, by Corollary 4, the *gros facteur* is never negative, thus, if there exists a point where the *gros facteur* vanishes, it is a local minimum of the *gros facteur* and thus all its partial derivatives (with respect to $\{a,x,y,\alpha,\beta\}$) are zero. □

Note that Lemma 5 says, in other words, that the zeros of $\Delta$ are the singular points[5] of the *gros facteur*.

We now state our main lemma which implies that the discriminant is zero only if a simple condition is satisfied.

**Main Lemma** *The discriminant $\Delta$ is equal to zero only if $y+a\alpha=0$ or $ax+\beta=0$.*

**Proof.** By Lemma 5, $\Delta$ is zero if and only if the *gros facteur* and all its partial derivatives are zero. We prove below that this implies that $(y+a\alpha)\,(ax+\beta)\,(1+\alpha^2+\beta^2)\,\Gamma = 0$, where

$$\Gamma = \left(2a\,(y\alpha-\beta x)-a^2+1\right)^2+3\,(ax+\beta)^2+3a^2\,(y+a\alpha)^2+3\,\left(1+a^2\right)^2. \tag{4}$$

[4] As an example where the set is not empty, we also present, in Table 1, the result of the computation of at least one point in every connected component of the set of $\chi \in \mathbb{R}^6$ such that $\mathcal{D}(\chi) > 0$.

[5] Recall that the singular points of a surface are the points where all partial derivatives are zero.

As the two terms $(1+\alpha^2+\beta^2)$ and $\Gamma$ clearly do not have any real solutions, this proves the lemma. (We discuss later how we found these terms.)

Consider the system in the variables $\{a,x,y,\alpha,\beta,u,v,w,t\}$ that consists of the *gros facteur*, its partial derivatives, and the four equations

$$1-u(y+a\alpha)=0, \quad 1-v(ax+\beta)=0, \quad 1-w(1+\alpha^2+\beta^2)=0, \quad 1-t\Gamma=0. \tag{5}$$

The *gros facteur* and its partial derivatives have a common zero (real or complex) such that $(y+a\alpha)(ax+\beta)(1+\alpha^2+\beta^2)\Gamma \neq 0$ if and only if this system has a solution. This follows immediately from the fact that the equations (5) are linear in $u,v,w,t$.

The Gröbner basis of that system is reduced to the polynomial 1 (see Table 2) and thus the system has no solution (over the complexes). This concludes the proof. □

The real difficulty in the proof of the Main Lemma is, of course, to find the equations (5) that rule out all the imaginary components of the set of singular points of the *gros facteur*. Computing these components is the actual key of the proof. We believe that the technique we used can be of some interest to the community as it is rather generic and could be applied to other problems. We thus describe in Section 2.3 how these components were computed before finishing the study of the algebraic structure of the trisector, in Section 2.4.

### 2.3 About the proof of the Main Lemma

We show in this section how we computed, for the proof of the Main Lemma, the equations of (5) which correspond to hypersurfaces containing the zeros of the discriminant.

Basically, we proceed as follows. We start from the system of equations of the *gros facteur* and all its partial derivatives and use the following techniques to study its set of solutions, or more precisely to decompose it into components defined by prime ideals[6]. This could theoretically be done by a general algorithm computing such a decomposition, however, all existing implementations are far from being capable of handling our particular problem or even a simpler sub-problem (see Remark 6).

If the (reduced) Gröbner basis of some system contains a polynomial which has a factor, say $F$, the solutions of the system splits into two components, one of which such that $F=0$, the other such that $F\neq 0$. We study separately the two components. One is obtained by adding the equation $F$ to the system and the other is obtained by adding the equation $1-tF$ and eliminating the variable $t$; indeed, there is a one-to-one correspondence between the solutions of the initial system such that $F\neq 0$ and the solutions of the system augmented by $1-tF$. Sometimes, frequently in our case, the component $F\neq 0$ is empty, which corresponds to the situation where the elimination of $t$ results in the polynomial 1 (inducing the equation $1=0$). Note that in some cases the system contains a polynomial which is a square, say $F^2$, thus the component such that $F\neq 0$ is obviously empty and we can add $F$ to the system without changing its set of solutions (this however changes the ideal). This operation of adding $F$ to the system frequently adds embedded components to the variety of solutions which explains why, later on in the process, empty components are frequently encountered when splitting into two components.

Our computations, presented in Table 3, are performed in Maple [22] using the Gröbner basis package FGb developed by J.-C. Faugère [15] . We use two functions,

*fgb_gbasis(sys,0,vars1,vars2)* and *fgb_gbasis_elim(sys,0,var1,var2)*[7],

that compute Gröbner bases of the system *sys*; the first uses a degree reverse lexicographic order (DRL) by blocks on the variables of *vars1* and *vars2* (where *vars2* is always the empty set in our computation) and the

[6] An ideal $I$ is prime if $PQ\in I$ implies $P\in I$ or $Q\in I$.

[7] The function *gbasis(sys,DRL(var1,var2),elim)* with or without the optional last argument *elim* can also be used alternatively of these two functions

second one eliminates the variable *vars1* and uses a reverse lexicographic order on the variables of *vars2*. (The second parameter of the functions refer to the characteristic of the field, here 0.)

We do not show in Table 3 the Gröbner bases which are too large to be useful, except in the case where the basis is reduced to 1 (when the system has no solution). We instead only report the first operand of each polynomial of the base; an operand $\star$ means that the polynomial is the product of at least two factors; an operand $\hat{}$ means that the polynomial is a power of some polynomial; an operand $+$ means that the polynomial is a sum of monomials.

Our computation goes as follows. We first simplify our system by considering $a = 2$ because otherwise the Gröbner basis computations are too slow and use too much memory to be performed successfully. We first see after computing, $bs_1$, the Gröbner basis of our system, that $y+2\alpha$ appears as a factor of one polynomial. This splits the solutions into those such that $y+2\alpha = 0$ and the others. We will study separately (in Lemma 7) the former set of solutions and we only consider here the solutions such that $y+2\alpha \neq 0$. This is done by adding the polynomial $1-u(y+2\alpha)$ to the system, where $u$ is a new variable; indeed there is a one-to-one correspondence between the solutions of the initial system such that $y+2\alpha \neq 0$ and the solutions of the resulting system.

The term $y+2\alpha$ corresponds fairly clearly to the polynomial $y+a\alpha$ with $a = 2$, and because of the symmetry of our problem we also study separately the solutions such that $ax+\beta = 0$. Since we assumed $a = 2$, we only consider here the solutions such that $2x+\beta \neq 0$, by adding to the system the polynomial $1-v(2,x+\beta)$. Finally, we also add $1-w(1+\alpha^2+\beta^2)$ to the system, without changing its set of real of real roots; we do this because the term $1+\alpha^2+\beta^2$ appears in the leading coefficient of $\mathcal{D}(\lambda)$ which suggests that some component of solutions (without any real point) might be included in $1+\alpha^2+\beta^2$. (It should be noted that adding this polynomial to the system changes the resulting Gröbner basis, which shows that this addition indeed removes some imaginary component from the system.) We compute the Gröbner basis, $bs_2$, of that system, eliminating the variables $u, v, w$, which gives a system of four polynomials of degree six.

We then compute the Gröbner basis of $bs_2$, eliminating the variable $x$. This gives a basis $bs_3$ which is reduced to one polynomial of the form $P^2$. We thus add $P$ to the system $bs_2$ (we do not add it to $bs_3$ since $bs_3$ does not depend on $x$). The Gröbner basis, $bs_4$, of the new system contains several polynomials that are products of factors. We see that if we add to the system the constraint that the third factor of the first polynomial is not zero, the resulting system has no solution. We thus add this factor to the system and compute its Gröbner basis $bs_5$. We operate similarly to get $bs_6$. The basis $bs_6$ contains no product or power and we compute its Gröbner basis, $bs_7$, eliminating $y$ (eliminating $x$ gives no interesting basis). The last polynomial of $bs_7$ is a power and we proceed as before to get $bs_8$. We proceed similarly until we get to the basis $bs_{12}$.

The basis $bs_{12}$ consists of three polynomials of degree four (which is a simplification over $bs_2$ which consists of four polynomials of degree six). We observe that the last polynomial of $bs_{12}$ is

$$\Gamma_2 = (4y\alpha - 4\beta x - 3)^2 + 3(2x+\beta)^2 + 12(y+2\alpha)^2 + 75,$$

which is always positive over the reals.

We have thus proved that all the complex solutions, such that $a = 2$, of the initial system (the *gros facteur* and all its partial derivatives) satisfy $(1+\alpha^2+\beta^2)(y+2\alpha)(2x+\beta)\Gamma_2 = 0$.

Finally, to get the polynomial $\Gamma$ of Formula (4), we performed the same computation with $a = 3$ and $a = 5$ and *guessed* $\Gamma$ as an interpolation of the polynomials $\Gamma_2$, $\Gamma_3$, and $\Gamma_5$.

Note that all the computation for a fixed $a$ takes roughly eight minutes of elapsed time on a regular PC.

**Remark 6** *All the computations from $bs_2$ to $bs_{12}$ amounts to finding polynomials that have a power which is a combination of the elements of $bs_2$ (i.e. which are in the radical of the ideal generated by $bs_2$). Thus these computations would be advantageously replaced by a program computing the radical of an ideal*[8]*. Unfortunately, all available such programs fail on the ideal generated by $bs_2$ either by exhausting the memory or by*

[8]The radical of an ideal $I$ is the ideal $\{x \mid x^n \in I \text{ for some } n \in \mathbb{N}\}$.

*running unsuccessfully during several days and ending on an error. It is therefore a challenge to improve these programs so that they are able to automatically do this computation.*

## 2.4 Algebraic structure of the trisector, Part II

**Lemma 7** *The discriminant $\Delta$ is equal to zero if and only if*

$$y = -a\alpha \quad \textit{and} \quad x = \frac{\beta(2a^2+1) \pm 2\sqrt{a^2(1+a^2)(\alpha^2+\beta^2+1)}}{a}, \quad \textit{or} \tag{6}$$

$$x = -\frac{\beta}{a} \quad \textit{and} \quad y = \frac{\alpha(2+a^2) \pm 2\sqrt{(1+a^2)(\alpha^2+\beta^2+1)}}{a}. \tag{7}$$

**Proof.** We refer to Table 5, Appendix F, for the computations. By the Main Lemma, $\Delta = 0$ implies $y + a\alpha = 0$ or $ax + \beta = 0$. Substituting $y$ by $-a\alpha$ in $\Delta$ gives an expression of the form $f_0 f_1^2$. Similarly, substituting $x$ by $-\beta/a$ in $\Delta$ gives an expression of the form $g_0 g_1^2$ (recall that $a \neq 0$ since the lines are not coplanar, by assumption). It follows that $\Delta = 0$ if and only if $y + a\alpha = f_i = 0$ or $ax + \beta = g_i = 0$, for $i = 0$ or 1. The $f_i$ and $g_i$ are polynomials of degree two in $x$ and $y$, respectively. Solving $f_1 = 0$ in terms of $x$ directly yields that the system $y + a\alpha = f_1 = 0$ is equivalent to (6). Similarly, solving $g_1 = 0$ in terms of $y$ yields (7). On the other hand, we prove that the solutions of $y + a\alpha = f_0 = 0$ and $ax + \beta = g_0 = 0$ are included in the set of solutions of (7) and (6), respectively, which concludes the proof. Because of lack of space, we omit here this proof (see Appendix A for a complete proof). □

**Lemma 8** *If $\Delta = 0$, the trisector of $\ell_1, \ell_2$, and $\ell_3$ consists of a cubic and a line that do not intersect in real space.*

**Proof.** By Lemma 7, $\Delta = 0$ if and only if System (6) or (7) is satisfied. By symmetry of the problem (we omit here the specification of the symmetry) we only need to consider one of the components of (6) and (7). Hence, it is sufficient to show that the system $y = -a\alpha$, $x = \frac{\beta(2a^2+1)}{a} + 2\sqrt{(1+a^2)(\alpha^2+\beta^2+1)}$ implies that the trisector consists of a cubic and a line that do not intersect. We assume in the following that this system is satisfied and that $\Delta = 0$. We refer to Table 6 for the computations.

We first show that the characteristic polynomial of the pencil generated by the bisectors is always strictly positive. Recall that the characteristic polynomial is never negative (see Lemma 3). It is thus sufficient to prove that it is never zero, or equivalently, that its product with its algebraic conjugate (obtained by changing the sign of $\sqrt{(1+a^2)(\alpha^2+\beta^2+1)}$) is never zero. This product is a polynomial $T$ in $a, \alpha, \beta, \lambda$. We compute, similarly as in the proof of Lemma 3, at least one point per connected component of the real semi-algebraic set $\{\chi = (a, \alpha, \beta, \lambda) \in \mathbb{R}^4 \mid T(\chi) - \frac{1}{2} < 0\}$. The resulting set of points is empty, hence $T(\chi)$ is always greater or equal to $1/2$. It thus follows that the characteristic polynomial is always strictly positive.

Since the characteristic polynomial $\mathcal{D}(\lambda)$ is always strictly positive and its discriminant $\Delta$ is zero, $\mathcal{D}(\lambda)$ admits two (conjugate) double imaginary roots. Let $\lambda_1$ and $\lambda_2$ denote these two roots. Recall that $\mathcal{D}(\lambda) = \det P(\lambda)$ with $P(\lambda) = \lambda Q_{1,2} + Q_{1,3}$ where $Q_{i,j}$ is the matrix associated with the hyperbolic paraboloid $\mathcal{H}_{i,j}$. It follows from the classification of the intersection of quadrics [12, Table 4] that either (i) $P(\lambda_1)$ and $P(\lambda_2)$ are of rank 3 and the trisector $\mathcal{H}_{1,2} \cap \mathcal{H}_{1,3}$ consists of a cubic and a line that do not intersect or (ii) $P(\lambda_1)$ and $P(\lambda_2)$ are of rank 2 and the trisector consists of two secant lines.

We now prove that $P(\lambda_1)$ and $P(\lambda_2)$ are of rank 3. We compute the Gröbner basis of all the $3 \times 3$ minors of $P(\lambda)$ and of the polynomial $1 - t\Psi$ with

$$\Psi = (1+a^2)(1+\alpha^2+\beta^2)(ax - y - \beta + a\alpha)(y + ax - a\alpha - \beta).$$

The basis is equal to 1, thus the $3 \times 3$ minors of $P(\lambda)$ are not all simultaneously equal to zero when $\Psi \neq 0$. Furthermore, $\Psi \neq 0$ for any $x, y, a, \alpha, \beta$ in $\mathbb{R}$ such that the lines $\ell_1, \ell_2$, and $\ell_3$ are pairwise skew (see (2) and the

proof of Lemma 5). Thus the rank of $P(\lambda)$ is at least 3. The rank of $P(\lambda_i)$, $i = 1,2$, is thus equal to 3 since $\det P(\lambda_i) = 0$. We can thus conclude that when $\Delta = 0$ the trisector consists of a cubic and a line that do not intersect in real space. □

We now state a proposition that shows that the trisector admits four asymptotes that are pairwise skew and gives a geometric characterization of their directions.

**Proposition 9** *The trisector of $\ell_1, \ell_2$, and $\ell_3$ intersects the plane at infinity in four real simple points. Furthermore, the four corresponding asymptotes are parallel to the four trisector lines of three concurrent lines that are parallel to $\ell_1, \ell_2$, and $\ell_3$, respectively.*

**Proof.** The trisector is the intersection of two hyperbolic paraboloids. Any hyperbolic paraboloid contains two lines at infinity. Hence the intersection, at infinity, of any two distinct hyperbolic paraboloids is the intersection of two pairs of lines. The intersection of these two pairs of lines consists of exactly four simple real points unless the point of intersection of the two lines in one pair lies on one line of the other pair. Because of lack of space, we omit here the proof that this cannot happen under our assumptions and the characterization of the four asymptotes (see Appendix B for a complete proof). □

**Theorem 10** *The trisector of three lines in general position consists of four infinite smooth branches of a non-singular quartic or of a cubic and a line that do not intersect in real space.*

**Proof.** As mentioned in the beginning of Section 2.2, the trisector of tree lines consists of a smooth quartic unless the discriminant $\Delta$ is zero. Lemma 8 and Proposition 9 thus yield the result. □

### 2.5 Topology of the Voronoi diagram

We omit the proof of the following first lemma because of lack of space (see Appendix C for a proof).

**Lemma 11** *There is a one-to-one correspondence between the set of ordered triplets of lines (in general position) and the set of affine frames of positive orientation.*

**Corollary 12** *The set of triplets of lines in general position is connected.*

**Theorem 13** *The topology of the Voronoi diagram of three lines in general position is invariant.*

**Proof.** Consider three lines in general position and a bisector of two of them. The bisector is a hyperbolic paraboloid which is homeomorphic to a plane. The trisector lies on the bisector and it is homeomorphic to four lines that do not pairwise intersect, by Theorem 10. Hence the topology of the regions that lie on the bisector and are bounded by the trisector is invariant by continuous deformation on any connected set of triplets of lines (in general position). The topology of these regions is thus invariant by continuous deformation on the set of all triplets of lines in general position (by Corollary 12). It follows that the topology of the two-dimensional cells of the Voronoi diagram is invariant by such a continuous deformation. The Voronoi diagram is defined by the embedding in $\mathbb{R}^3$ of its two-dimensional cells, hence its topology is also invariant by continuous deformation. □

**Proof of Theorem 1.** Theorem 1 follows from Theorems 10 and 13 and from the computation of an example of a two-dimensional cell of the Voronoi diagram (for instance the one shown in Figure 1). □

## 3 Properties of the Voronoi diagram and algorithms

We present here some fundamental properties of the Voronoi diagram and algorithms for separating the two components of each two-dimensional Voronoi cell and the four components of the cell of dimension one. Because of the lack of space, we omit all proofs (see Appendix D for proofs). We start by presenting two

properties, one on the asymptotes of the trisector and one on the incidence relations between cells, which directly yield an unambiguous labeling of the components of the trisector.

Let $V_{ij}$ denote the Voronoi cell of lines $\ell_i$ and $\ell_j$ and let $U_{ij}$ and $T_{ij}$ denote the connected components of $V_{ij}$ that are bounded by one and three arcs of the trisector, respectively (see Figure 1).

**Proposition 14** *Exactly one of the four branches of the trisector of three lines in general position admits only one asymptote. Let $C_0$ denote this branch. Each cell $U_{ij}$ is bounded by a branch distinct from $C_0$ and every such branch bounds a cell $U_{ij}$.*

*Let $C_k$, $k = 1,2,3$, denote the branches of the trisector that bound the component $U_{ij}$, $i, j \neq k$. The labeling of the four branches of the trisector by $C_0, \ldots, C_4$ is unambiguous.*

Note that differentiating between $C_1$ and $C_2$ cannot be done by only looking at the cell $V_{12}$ (Figure 1) but has to be done by looking at the other cells $V_{13}$ and $V_{23}$. Differentiating between $C_1$ and $C_2$ on Figure 1 can be done by computing (using the algorithm described below) a vertical ordering (along the $Z$-axis) of the components $U_{ij}$ and $T_{ij}$ and determining the branch $C_k$ for which $U_{ij}$ appears only on side of the branch (see Figure 2(b)).

We now present two important properties of trisector of the Voronoi diagram of three lines $\ell_1$, $\ell_2$, and $\ell_3$ in general position and a simple algorithm for separating the two components of a two-dimensional Voronoi cell. We consider the $(X,Y,Z)$ frame described in Step (i) of the algorithm below.

**Proposition 15** *The orthogonal projection of the trisector of $\ell_1$, $\ell_2$, and $\ell_3$ onto the $XY$-plane has two asymptotes parallel to the $X$-axis and two asymptotes parallel to the $Y$-axis.*

**Proposition 16** *Every branch of the trisector of $\ell_1$, $\ell_2$, and $\ell_3$ is monotonic with respect to the $Y$-direction (or every branch is monotonic with respect to the $X$-direction).*

**Algorithm to compute a linear halfspace, $H_{ij}$, that contains $U_{ij}$ and whose complement contains $T_{ij}$.**

(i) Consider a Cartesian coordinate system $(X,Y,Z)$ such that the $Z$-axis is parallel to the common perpendicular of $\ell_i$ and $\ell_j$ and such that the $X$ and $Y$-axis are parallel to the two bisector lines, in a plane perpendicular to the $Z$-axis, of the projection of $\ell_i$ and $\ell_j$ onto that plane.

(ii) In this frame, compute all the critical values of the trisector with respect to the $X$-axis and with respect to the $Y$-axis. Exchange the $X$- and $Y$-axis if there is no critical value with respect to the $X$-axis.

(iii) Compute the two $X$-values of the two trisector asymptotes parallel to the $XZ$-plane. If the minimum of these values is smaller than the smaller critical value, then change the orientation of the three axes.

(iv) Compute a value $\tilde{x}$ larger than the smaller critical value and smaller that all the other critical values and the two asymptote $X$-values. The halfspace, $H_{ij}$, of equation $X < \tilde{x}$ contains $U_{ij}$ and the halfspace $X > \tilde{x}$ contains $T_{ij}$.

This linear semi-algebraic test for separating the components $U_{ij}$ and $T_{ij}$ and Proposition 14 gives directly a linear semi-algebraic test for separating the components of the trisector.

**Proposition 17** *For any point $p$ on the trisector, if $p$ belongs to a halfspace $H_{ij}$, then it lies on $C_k$, otherwise, if $p$ belongs to none of the $H_{ij}$, it lies on $C_0$.*

Finally, the above algorithm and Propositions 16 and 17 give Theorem 2.

# 4 Configurations of three lines whose trisector contains a line

We present here a geometric characterization of the position of three lines in general position such that their trisector contains a line (i.e., consists of a cubic and line). We show that, if the trisector of three lines in general position contains a line, then the center $O$ of a parallelepiped associated to the lines is on the trisector line which is the line through $O$ and parallel to the interior trisector of an associated frame. Because of lack of space, we omit here the description of the parallelepiped and frame (which are the ones of Lemma 11), the precise meaning of interior trisector, and all proofs (see Appendix E for details). Conversely, we also show that if the direction of the lines are not in some special configuration, then the trisector contains a line if and only if it contains the center of the associated parallelepiped.

## References


[1] F. Aurenhammer. Voronoi diagrams – a survey of a fundamental geometric data structure. *ACM Computing Surveys*, 23(3):345–405, 1991.

[2] F. Aurenhammer and R. Klein. Voronoi diagrams. In J. R. Sack and J. Urrutia, editors, *Handbook of computational geometry*, chapter 5, pages 201–290. Elsevier Publishing House, December 1999.

[3] E. Berberich, M. Hemmer, L. Kettner, E. Schömer, and N. Wolpert. An exact, complete and efficient implementation for computing planar maps of quadric intersection curves. In *Proceedings of the 21th ACM Annual Symposium on Computational Geometry (SoCG'05)*, pages 99–115, 2005.

[4] J.-D. Boissonnat, O. Devillers, S. Pion, M. Teillaud, and M. Yvinec. Triangulations in CGAL. *Computational Geometry: Theory and Applications*, 22:5–19, 2002.

[5] J.-D. Boissonnat, O. Devillers, R. Schott, M. Teillaud, and M. Yvinec. Applications of random sampling to on-line algorithms in computational geometry. *Discrete and Computational Geometry*, 8:51–71, 1992.

[6] T. M. Chan, J. Snoeyink, and C. K. Yap. Primal dividing and dual pruning: Output-sensitive construction of four dimensional polytopes and three-dimensional diagram voronoi diagrams. *Discrete and Computational Geometry*, 18:433–454, 1997.

[7] K. L. Clarkson and P. W. Shor. Applications of random sampling in computational geometry, II. *Discrete and Computational Geometry*, 4:387–421, 1989.

[8] H. Cohen. *A course in computational algebraic number theory*, volume 138 of *Graduate Texts in Mathematics*. Springer-Verlag, 3-rd edition, Berlin, 1996.

[9] T. Culver. *Computing the Medial Axis of a Polyhedron Reliably and Efficiently*. PhD thesis, University of North Carolina at Chapel Hill, 2000.

[10] T. K. Dey and W. Zhao. Approximate medial axis as a voronoi subcomplex. In *SMA '02: Proceedings of the seventh ACM symposium on Solid modeling and applications*, pages 356–366, New York, NY, USA, 2002. ACM Press.

[11] L. Dupont, D. Lazard, S. Lazard, and S. Petitjean. Near-optimal parameterization of the intersection of quadrics: I. The generic algorithm. Research Report n$^o$ 5667, INRIA, Sept. 2005. 36 pages.

[12] L. Dupont, D. Lazard, S. Lazard, and S. Petitjean. Near-optimal parameterization of the intersection of quadrics: II. A classification of pencils. Research Report n$^o$ 5668, INRIA, Sept. 2005. 37 pages.

[13] M. Etzion and A. Rappoport. Computing voronoi skeletons of a 3-d polyhedron by space subdivision. *Computational Geometry: Theory and Applications*, 21(3):87–120, 2002.

[14] S. Fortune. Voronoi diagrams and delaunay triangulations. In *Handbook of discrete and computational geometry*, pages 377–388. CRC Press, Inc., Boca Raton, FL, USA, 1997.

[15] Gb/FGb. J.-C. Faugre. `http://fgbrs.lip6.fr`.

[16] K. Hoff, T. Culver, J. Keyser, M. Lin, and D. Manocha. Fast computation of generalized Voronoi diagrams using graphics hardware. *Computer Graphics*, 33(Annual Conference Series):277–286, 1999. Proceedings of ACM SIGGRAPH 1999.

[17] M. I. Karavelas. A robust and efficient implementation for the segment voronoi diagram. In *International Symposium on Voronoi Diagrams in Science and Engineering*, pages 51–62, 2004.

[18] J. Keyser, S. Krishnan, and D. Manocha. Efficient and accurate B-Rep generation of low degree sculptured solids using exact arithmetic: I – Representations, II – Computation. *Computer Aided Geometric Design*, 16(9):841–859, 861–882, 1999.

[19] V. Koltun and M. Sharir. Three dimensional euclidean voronoi diagrams of lines with a fixed number of orientations. *SIAM Journal on Computing*, 32(3):616–642, 2003.

[20] K. Kurdyka, P. Orro, and S. Simon. Semialgebraic Sard theorem for generalized critical values. *Journal of Differential Geometry*, 56:67–92, 2000.

[21] D. Leven and M. Sharir. Intersection and proximity problems and voronoi diagrams. In J. T. Schwartz and C.-K. Yap, editors, *Advances in Robotics 1: Algorithmic and Geometric Aspects of Robotics*, pages 187–228. Lawrence Erlbaum Associates, Hillsdale, NJ, 1987.

[22] The Maple System. Waterloo Maple Software. `http://www.maplesoft.com`.

[23] V. J. Milenkovic. Robust construction of the voronoi diagram of a polyhedron. In *Proceedings of 5th Canadian Conference on Computational Geometry (CCCG'93)*, pages 473–478, 1993.

[24] B. Mourrain, J.-P. Técourt, and M. Teillaud. On the computation of an arrangement of quadrics in 3D. *Computational Geometry: Theory and Applications*, 30(2):145–164, 2005. Special issue, 19th European Workshop on Computational Geometry.

[25] A. Okabe, B. Boots, K. Sugihara, and S. N. Chiu. *Spatial Tessellations - Concepts and Applications of Voronoi Diagrams*. John Wiley, 2nd edition, 2000.

[26] RAG'Lib: A Library for real algebraic geometry. M. Safey El Din, 2003. `http://www-calfor.lip6.fr/~safey/RAGLib/`.

[27] F. Rouillier, M.-F. Roy, and M. Safey El Din. Finding at least one point in each connected component of a real algebraic set defined by a single equation. *Journal of Complexity*, 16:716–750, 2000.

[28] M. Safey El Din. Generalized critical values and testing sign conditions on a polynomial. In D. Wang and Z. Zheng, editors, *Proceedings of Mathematical Aspects of Computer and Information Science*, pages 61–84. 2006.

[29] M. Safey El Din and E. Schost. Polar varieties and computation of at least one point in each connected component of a smooth real algebraic set. In *Proceedings of the International Symposium on Symbolic and Algebraic Computation (ISSAC'03)*, pages 224–231, Philadelphia PA, 2003. ACM Press.

[30] M. Safey El Din and E. Schost. Properness defects of projections and computation of one point in each connected component of a real algebraic set. *Discrete and Computational Geometry*, 32(3):417–430, 2004.

[31] E. Schömer and N. Wolpert. An exact and efficient approach for computing a cell in an arrangement of quadrics. *Computational Geometry: Theory and Applications*, 33(1-2):65–97, 2006. Special Issue on Robust Geometric Algorithms and their Implementations.

[32] O. Schwarzkopf and M. Sharir. Vertical decomposition of a single cell in a three-dimensional arrangement of surfaces and its applications. *Discrete and Computational Geometry*, 18:269–288, 1997.

[33] C. Segre. Studio sulle quadriche in uno spazio lineare ad un numero qualunque di dimensioni. *Mem. della R. Acc. delle Scienze di Torino*, 36(2):3–86, 1883.

[34] R. Seidel. A convex hull algorithm optimal for point sets in even dimensions. M.Sc. thesis, Univ. British Columbia, Vancouver, BC, 1981. Report 81/14.

[35] M. Sharir. Almost tight upper bounds for lower envelopes in higher dimensions. *Discrete and Computational Geometry*, 12:327–345, 1994.

[36] M. Teichmann and S. Teller. Polygonal approximation of voronoi diagrams of a set of triangles in three dimensions. Technical Report 766, Laboratory of Computer Science, MIT, 1997.

# A Proof of Lemma 7

We give here a complete proof of Lemma 7 which states:

*The discriminant $\Delta$ is equal to zero if and only if*

$$y = -a\alpha \quad \textit{and} \quad x = \frac{\beta(2a^2+1) \pm 2\sqrt{a^2(1+a^2)(\alpha^2+\beta^2+1)}}{a}, \quad \textit{or} \tag{6}$$

$$x = -\frac{\beta}{a} \quad \textit{and} \quad y = \frac{\alpha(2+a^2) \pm 2\sqrt{(1+a^2)(\alpha^2+\beta^2+1)}}{a}. \tag{7}$$

We refer to Table 5, Appendix F, for the computations. Recall that, by the Main Lemma, $\Delta = 0$ implies $y + a\alpha = 0$ or $ax + \beta = 0$. Substituting $y$ by $-a\alpha$ in $\Delta$ gives an expression of the form $f_0 f_1^2$. Similarly, substituting $x$ by $-\beta/a$ in $\Delta$ gives an expression of the form $g_0 g_1^2$ (recall that $a \neq 0$ since the lines are not coplanar, by assumption). It follows that $\Delta = 0$ if and only if $y + a\alpha = f_i = 0$ or $ax + \beta = g_i = 0$, for $i = 0$ or 1.

Recall also that the $f_i$ and $g_i$ are polynomials of degree two in $x$ and $y$, respectively, and that solving $f_1 = 0$ in terms of $x$ directly yields that the system

$$y + a\alpha \quad = \quad f_1 \quad = \quad 0 \tag{8}$$

is equivalent to (6). Similarly, solving $g_1 = 0$ in terms of $y$ yields that the system

$$ax + \beta \quad = \quad g_1 \quad = \quad 0 \tag{9}$$

is equivalent to (7).

We now show that the solutions of $y + a\alpha = f_0 = 0$ are included in the set of solutions of (7). The polynomial $f_0$ is the sum of two squares. It follows that $y + a\alpha = f_0 = 0$ if and only if

$$y + a\alpha \quad = \quad a^2\alpha^2 - 1 + a\beta x \quad = \quad ax + \beta \quad = \quad 0. \tag{10}$$

We show below that the polynomials of (9) are included in the ideal generated by the polynomials of (10). This implies that (9) is, roughly speaking, less constrained than (10) and that the set of solutions of (9) contains the solutions of (10). Hence the solutions of $y + a\alpha = f_0 = 0$ are contained in the set of solutions of (9) and thus in the set of solutions of (7).

We prove that the polynomials of (9) are included in the ideal generated by the polynomials of (10) by showing that the normal form of every polynomial of (9) with respect to the Gröbner basis of the polynomials of (10) is zero. This is done using the function *normalf* (of Maple) which computes the normal form of a polynomial with respect to a Gröbner basis.

We prove similarly that the solutions of $ax + \beta = g_0 = 0$ are included in the set of solutions of (8) and thus of (6), which concludes the proof.

# B Proof of Proposition 9

We prove here Proposition 9 which state:

*The trisector of $\ell_1, \ell_2$, and $\ell_3$ intersects the plane at infinity in four real simple points. Furthermore, the four corresponding asymptotes are parallel to the four trisector lines of three concurrent lines that are parallel to $\ell_1, \ell_2$, and $\ell_3$, respectively.*

The intersection with the plane at infinity of the bisector of lines $\ell_1$ and $\ell_2$ consists of the lines at infinity in the pair of planes of equation $XY = 0$ (the homogeneous part of highest degree in the equation of the bisector of lines $\ell_1$ and $\ell_2$ which is equal to $Z = -\frac{a}{1+a^2}XY$). This pair of planes is the bisector of the two concurrent lines that are parallel to $\ell_1$ and $\ell_2$, respectively. Note that the lines at infinity in this pair of planes are invariant by translation of the planes. We thus get that the lines at infinity of the bisector of any two lines $\ell_i$ and $\ell_j$ are the lines at infinity in the pair of planes that is the bisector to any two concurrent lines that are parallel to $\ell_i$ and $\ell_j$, respectively.

It follows that the points at infinity on the trisector of $\ell_1, \ell_2$, and $\ell_3$ are the points at infinity on the trisector lines (the intersection of bisector planes) of three concurrent lines that are parallel to $\ell_1, \ell_2$, and $\ell_3$, respectively. It remains to show that this trisector consists of four distinct lines.

Let $\ell'_1$, $\ell'_2$, and $\ell'_3$ be the three concurrent lines through the origin that are parallel to $\ell_1$, $\ell_2$, and $\ell_3$, respectively, and suppose, for a contradiction, that their trisector does not consist of four distinct lines. This implies that the line of intersection of the two bisector planes of two lines, say $\ell'_1$ and $\ell'_2$, is contained in one of the bisector planes of two other lines, say $\ell'_1$ and $\ell'_3$. The intersection of the bisector planes of $\ell'_1$ and $\ell'_2$ is the $Z$-axis. It follows that one of the bisector planes of $\ell'_1$ and $\ell'_3$ is vertical, hence $\ell'_1$ and $\ell'_3$ are symmetric with respect to a vertical plane and thus $\ell'_3$ is contained in the $XY$-plane. Therefore, $\ell'_1$, $\ell'_2$, and $\ell'_3$ lie in the $XY$-plane, contradicting the general position assumption, which concludes the proof.

# C Proof of Lemma 11

We prove here Lemma 11 which states:

> *There is a one-to-one correspondence between the set of ordered triplets of lines (in general position) and the set of affine frames of positive orientation.*

Consider three lines $\ell_1, \ell_2$, and $\ell_3$ in general position and refer to Figure 3. For the three choices of pairs of lines $\ell_i, \ell_j$, consider the plane containing $\ell_i$ and parallel to $\ell_j$, the plane containing $\ell_j$ and parallel to $\ell_i$, and the region bounded by these two parallel planes. The general position assumption implies that these regions have non-empty interiors and that no three planes are parallel. The intersection of these three regions thus defines a parallelepiped. By construction, each of the lines $\ell_1, \ell_2$, and $\ell_3$ contains an edge of that parallelepiped. These lines are pairwise skew thus exactly two vertices of the parallelepiped are not on the lines. Each of these two points induces an affine frame centered at the point and with basis the three edges of the parallelepiped oriented from the point to the lines $\ell_1, \ell_2$, and $\ell_3$, in this order. One of the points ($C$ on the figure) defines a frame of positive orientation, the other defines a frame of negative orientation ($C'$ on the figure). This construction exhibits a one-to-one correspondence between the set of ordered triplets of lines (in general position) and the set of affine frames of positive orientation, which concludes the proof.

# D Proofs of Section 3: Properties of the Voronoi diagram and algorithms

We present here the missing proofs of Section 3. We first prove three lemmas that, together, prove Proposition 14.

**Lemma 18** *Exactly one of the four branches of the trisector of three lines in general position admits only one asymptote.*

**Proof.** By Proposition 9, the trisector admits four *simple* asymptotes, for all triplets of lines in general position. It follows that the property that exactly one of the branches of the trisector has only one asymptote is invariant by continuous deformation on the set of triplets of lines in general position. The result thus follows from Corollary 12 and from the observation that the property is verified on one particular example (see Fig 1). □

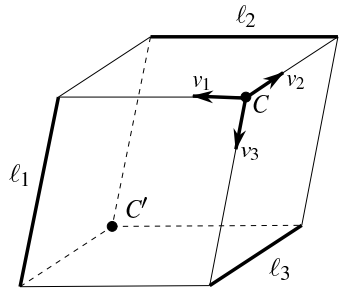


Figure 3: The parallelepiped formed by $\ell_1$, $\ell_2$, and $\ell_3$ and the associated frame $(C, v_1, v_2, v_3)$ of positive orientation.

We denote by $C_0$ the branch of the trisector that admits only one asymptote (see Figure 1), and $C_1$, $C_2$, and $C_3$ the three others (the ordering of these three branches is, for the moment, arbitrary).

Let $V_{ij}$ denote the Voronoi cell of lines $\ell_i$ and $\ell_j$. Let $U_{ij}$ and $T_{ij}$ denote the connected components of $V_{ij}$ that are bounded by one and three arcs of the trisector, respectively (see Figure 1).

**Lemma 19** *Each cell $U_{ij}$ is bounded by a branch $C_k$, $k = 1,2,3$, and every such branch bounds a cell $U_{ij}$.*

**Proof.** This property is invariant by continuous deformation on the set of triplets of lines in general position. It is thus sufficient to prove it for any three given lines in general position, $\ell_1, \ell_2, \ell_3$, as defined in Section 2.1. We consider in the $XY$-plane the arrangement of the (orthogonal) projection of the trisector and of the silhouette curves (viewed from infinity in the $Z$-direction) of the bisectors (see Figure 2(b)); these silhouette curves consist of only two parabolas since the bisector of lines $\ell_1$ and $\ell_2$ has no such silhouette (its equation has the form $Z = cstXY$ and thus any vertical line intersects it). By construction, for all vertical lines intersecting one given (open) cell of this arrangement, the number and ordering of the intersection points between the vertical line and all the pieces of the three bisectors that are bounded by the trisector is invariant. For any point of intersection, we can easily determine (by computing distances) whether the point lies on a Voronoi cell $V_{ij}$. We can further determine whether the point belongs to the component $U_{ij}$ or $T_{ij}$ by using the linear separation test described below. We thus report the ordering of the components $U_{ij}$ and $T_{ij}$ above each cell of the arrangement in the $XY$-plane for a given example; see Figure 2(b).

We can now observe that there is a one-to-one correspondence between the three branches $C_1$, $C_2$, and $C_3$ and the components $U_{12}$, $U_{13}$, and $U_{23}$ such that the component appears only on one side of the corresponding branch[9]. It follows that each of the branches $C_1$, $C_2$, and $C_3$ bounds a cell $U_{ij}$. □

Since $U_{ij}$ is, by definition, bounded by only one arc of the trisector, Lemmas 18 and 19 directly yield the following property.

**Lemma 20** *Let $C_0$ denote the only branch of the trisector that admits only one asymptote and $C_k$, $k = 1,2,3$, denote the branches of the trisector that bound the component $U_{ij}$, $i, j \neq k$ (see Figure 1). This labeling of the four branches of the trisector by $C_0, \ldots, C_4$ is unambiguous.*

We now consider any three lines $\ell_1$, $\ell_2$, and $\ell_3$ in general position (pairwise skew and not all parallel to a common plane) and an associated Cartesian coordinate system $(X,Y,Z)$ such that the $Z$-axis is parallel to the common perpendicular of $\ell_1$ and $\ell_2$ and such that the $X$ and $Y$-axis are parallel to the two bisector lines, in a plane perpendicular to the $Z$-axis, of the projection of $\ell_1$ and $\ell_2$ onto that plane.[10] Note that the orientations of

[9] Namely, $U_{13}$ (resp. $U_{23}$ and $U_{12}$) appears on only one side of the lower-right (resp. upper-right and left-most) branch.

[10] Note that this setting is slightly different than the one described in Section 2.1 since, here, any triplet of three lines in general position can be moved continuously into another while the associated frame moves continuously; however, if the initial and final triplets of lines are in the setting of Section 2.1, it is not necessarily possible to ensure that, during the motion, all triplets of lines remain in this setting.

the axis are not specified (except for the fact that the frame has a positive orientation) and that the $X$ and $Y$-axis can be exchanged. We now prove Proposition 15 which states:

> *The orthogonal projection of the trisector of $\ell_1$, $\ell_2$, and $\ell_3$ onto the $XY$-plane has two asymptotes parallel to the $X$-axis and two asymptotes parallel to the $Y$-axis.*

**Proof of Proposition 15.** By proposition 9, the four asymptotes of the trisector are parallel to the four trisector lines of three concurrent lines parallel to $\ell_1$, $\ell_2$, and $\ell_3$. The bisector to two lines through the origin and parallel to $\ell_1$ and $\ell_2$ is the pair of planes of equation $XY = 0$. Hence the asymptotes of the trisector are parallel to lines that lie in the pair of planes $XY = 0$. The orthogonal projection of the asymptotes on the $XY$-plane are thus parallel to the $X$- or $Y$-axis. It follows that the number of asymptotes (in projection) that are parallel to the $X$-axis (resp. $Y$-axis) is invariant by continuous deformation on any connected set of triplets of lines in general position. The result follows from the fact that, on a particular example (see Figure 1), there are two asymptotes parallel to the $X$-axis and two others parallel to the $Y$-axis and that the set of triplets of lines in general position is connected (Corollary 12). □

We assume in the following that *the asymptote of $C_0$ is parallel to the $YZ$-plane* (as in Figure 1) by exchanging, if necessary, the role of $X$ and $Y$. We now prove Proposition 16 which states:

> *Every branch of the trisector of $\ell_1$, $\ell_2$, and $l_3$ is monotonic with respect to the $Y$-direction.*

**Proof of Proposition 16.** Let $\mathcal{P}$ denote any plane parallel to the $XZ$-plane. The arc $C_0$ intersects plane $\mathcal{P}$ an odd number of times (counted with multiplicity) since $C_0$ has only one asymptote (Proposition 14) which is parallel to the $YZ$-plane. Furthermore, by Proposition 15, the trisector has two other asymptotes parallel to the $XZ$-plane. Hence plane $\mathcal{P}$ intersects the trisector in two points at infinity and $C_0$ an odd number of times (in affine space). The trisector thus intersects $\mathcal{P}$ in at least three points in real projective space. There are thus four intersection points (in real projective space) since there are four intersection points in complex space (since the trisector is of degree four) and if there was an imaginary point of intersection, its conjugate would also be an intersection point (since the equations of the plane and quadrics have real coefficients) giving five points of intersection.

Therefore the trisector intersects plane $\mathcal{P}$ in two points in $\mathbb{R}^3$, one of which lies on $C_0$. Since there are an odd number of intersection points on $C_0$, plane $\mathcal{P}$ intersects $C_0$ exactly once and any other branch exactly once. □

We now prove the correctness of the algorithm, presented in Section 3, which we recall here for clarity.

**Algorithm for computing a linear halfspace, $H_{ij}$, that contains $U_{ij}$ and whose complement contains $T_{ij}$.**

(i) Consider a Cartesian coordinate system $(X,Y,Z)$ such that the $Z$-axis is parallel to the common perpendicular of $\ell_i$ and $\ell_j$ and such that the $X$ and $Y$-axis are parallel to the two bisector lines, in a plane perpendicular to the $Z$-axis, of the projection of $\ell_i$ and $\ell_j 2$ onto that plane.

(ii) In this frame, compute all the critical values of the trisector with respect to the $X$-axis and with respect to the $Y$-axis. Exchange the $X$- and $Y$-axis if there is no critical value with respect to the $X$-axis.

(iii) Compute the two $X$-values of the two trisector asymptotes parallel to the $XZ$-plane. If the minimum of these values is smaller than the smallest critical value, then change the orientation of the three axes.

(iv) Compute a value $\tilde{x}$ larger than the smaller critical value and smaller that all the other critical values and the two asymptote $X$-values. The halfspace, $H_{ij}$, of equation $X < \tilde{x}$ contains $U_{ij}$ and the halfspace $X > \tilde{x}$ contains $T_{ij}$.

**Proof of correctness.** For simplicity, we assume without loss of generality that $i$ and $j$ are equal to 1 and 2, respectively. By Proposition 16, the trisector has no critical point in the $X$ or $Y$-direction. Since we exchange,

in Step (ii), the $X$- and $Y$-axis if there is no critical value with respect to the $X$-direction, we have that there is no critical point with respect to the $Y$-direction.

First note that the asymptotes of the trisector are never vertical (*i.e.,* parallel to the $Z$-axis) because otherwise, by Proposition 9 and since $\ell_1$ and $\ell_2$ are horizontal, the line $\ell_3$ would be horizontal (its direction would be the symmetric of the one of $\ell_1$ with respect to a vertical plane), contradicting the general position assumption.

It thus follows, since the directions of the asymptotes, projected on the $XY$-plane, are parallel to the $X$ or $Y$-axis (by Proposition 15) that the oriented directions of the asymptotes of the branches of the projected trisector are invariant (in the direction $\pm X$ or $\pm Y$) by continuous deformation on the set of triplets of lines in general position (which is connected by Corollary 12).

Hence, it follows from the analysis of one configuration (see Figure 1) that the two projected asymptotes of the branch $C_3$ have the same oriented direction. Thus $C_3$ has (at least) a critical point with respect to this direction, whith is thus $+X$ or $-X$ since there is no critical point with respect to the $Y$-axis. Assume that this direction is the $-X$ direction (as in Figure 1), by changing, if necessary, the orientation of the axis.

We also get from the configuration depicted in Figure 1 that two other projected branches of asymptote that are parallel to the $X$-axis are in the $+X$ direction.

Furthermore, the plane, $\mathcal{P}$, parallel to the $YZ$-plane through the critical point of $C_3$ does not intersect the trisector in any other intersect point in $\mathbb{R}^3$ because this intersection has multiplicity two, the plane intersects the trisector in two points at infinity (by Proposition 15), and the trisector has degree four (it is the intersection of two quadrics). The same argument (applied to another critical point) implies that $C_3$ has no other critical point and that the trisector has no critical value smaller that the one associated to the critical point of $C_3$.

Hence, plane $\mathcal{P}$ separates (except for the critical point) the branch $C_3$ from the other branches and the plane of equation $X = \tilde{x}$ strictly separates $C_3$ from the other branches and leaves $C_3$ to its left (in the direction $-Y$). Hence the halfspace $X < \tilde{x}$ contains $U_{12}$ and the halfspace $X > \tilde{x}$ contains $T_{12}$.

It remains to show that the orientation of the $X$-axis obtained in Step (iii) of the algorithm is the same as the one we have considered so far. Consider the two $X$-values of the two trisector asymptotes parallel to the $XZ$-plane. We prove that the maximum of these values is larger than the largest critical value. This implies the result since, if the orientation of the $X$-axis was its opposite, then it would be changed in Step (iii).

As before, by continuity and by analyzing one particular example, we have that two of the asymptotes of the branches of $C_1$ and $C_2$ have direction $+X$ (in projection) and the two others have direction $+Y$ and $-Y$. We consider here the trisector and its asymptotes in projection on the $XY$-plane and we refer to vertical, right and left in a standard way in the $(X,Y)$ frame. Suppose for a contradiction that there exists a critical point on $C_1 \cup C_2$ that is left of their vertical asymptote. Then a vertical line, $\mathcal{L}$, through this critical point would intersect the trisector at this point, with multiplicity two, and at two other points at infinity (by Proposition 15). However, since the critical point is right of the vertical asymptote of $C_1$ and $C_2$, line $\mathcal{L}$ intersects the trisector somewhere else (or with higher multiplicity), which is not possible since the trisector has degree four. □

Note finally that the trisector has generically four critical points with respect to the $X$-direction, one on $C_3$, one on $C_1 \cup C_2$ and two on $C_0$ since it has an asymptote parallel to the $Y$-axis (in projection). Furthermore, the trisector has no other critical points for the following reason. The projection (on the $XY$-plane) of the trisector is a curve of degree four. Furthermore, it has degree two in $X$ and degree two in $Y$ because the curve intersects any line parallel to the $X$- or $Y$-axis in at most two points since there are two other points of intersection at infinity (by Proposition 15). The critical points are points on the curve such that the curve's partial derivative with respect to $Y$ is zero. This partial derivative is of degree one in $Y$ and two in $X$, hence eliminating $Y$ in the curve's equation give an equation in $X$ of degree four.

## E Configurations of three lines whose trisector contains a line

We present here a geometric characterization of the position of three lines in general position such that their trisector consists of a cubic and line. We need some properties of the trisector of the concurrent lines supported by the three vectors of an affine frame (the frame described in Lemma 11, where the vectors are the edges of the parallelepiped of Figure 3 issued from $C$).

Let us consider a basis $(v_1, v_2, v_3)$ of the vector space $\mathbb{R}^3$ equipped with its Euclidean structure (the usual dot product relative to the canonical basis) and name $d_1, d_2, d_3$ the lines supported by $v_1, v_2, v_3$.

**Lemma 21** *The trisector of the lines $d_1, d_2, d_3$ supported by the vector basis $(v_1, v_2, v_3)$ consists in four lines or eight half lines passing through the origin.*

*Given a point $p$ different from the origin on this trisector, its dual coordinates $< p, v_1 >, < p, v_2 >, < p, v_3 >$ are non null. Thus their signs are constant on each of the eight half lines of the trisector. These signs induce a one to one correspondence between the half lines and the eight possibilities for a triplet of signs.*

**Proof.** The trisector being the intersection of two of the bisectors, which are pairs of orthogonal planes, the first assertion is immediate.

If $< p, v_1 >=< p, v_2 >=< p, v_3 >= 0$, then $p$ is orthogonal to the three vectors $v_1, v_2$ and $v_3$ and therefore null. If $< p, v_1 >= 0$ and $< p, v_2 > \neq 0$, then the projection of $p$ on the plane $(v_1, v_2)$ is not null, lies on the bisector line of $v_1$ and $v_2$ in this plane and is orthogonal to $v_1$. This is a contradiction since the bisector of two distinct concurrent lines is never orthogonal to one of them and this shows that all the $< p, v_i >$ are not null.

The last assertion is immediate for an orthogonal basis and follows for the other bases from the connexity of the set of all the bases of positive orientation. □

**Lemma 22** *With the same notation, if one branch of the trisector of the lines $d_1, d_2, d_3$ is in the plane $(v_1, v_2)$, then each of the planes $(v_1, v_3)$ and $(v_2, v_3)$ contains another branch of the trisector.*

**Proof.** As above, we may suppose, without loss of generality that $v_1 = (1, a, 0), v_2 = (1, -a, 0)$ and $v_3 = (\alpha, \beta, 1)$. The trisector is defined by the equation $XY = 0$ and a homogeneous equation of degree two in $X, Y, Z$. The hypothesis implies thus that the trisector contains either the point $(0, 1, 0)$ or $(1, 0, 0)$. Substituting in the second equations of the trisector, we find respectively $a^2(1 + \alpha^2) - \beta^2 = 0$ or $a^2\alpha^2 - \beta^2 - 1 = 0$, which characterize algebraically our hypothesis. Using the symmetry with respect to the plane $X = Y$, we may restrict ourselves to the first case.

Substituting $X = 1, Y = 0$ and $\beta = a\sqrt{1 + a^2}$ in the second equation of the trisector and solving the resulting equation in $Z$ shows that the points $(1, 0, -a + \sqrt{1 + a^2})$ and $(1, 0, -a - \sqrt{1 + a^2})$ belong to the trisector. A simple determinant computation shows that they lie respectively on the planes $(v_2, v_3)$ and $(v_1, v_3)$. □

**Definition 23** *We name* interior trisector *the line of the trisector of $d_1, d_2, d_3$ on which the three signs of the $< p, v_i >$ are equal.*

*We say that the configuration of the directions of the lines is* special *if the case of Lemma 22 occurs.*

Remark that the interior trisector is the axis of the cone of revolution circumscribing the three vectors $v_1, v_2, v_3$ and that the three other lines of the trisector are the axes of the circumscribing cones obtained by changing the sign of one of the $v_i$.

**Theorem 24** *If the trisector of three lines in general position contains a line, then the center $O$ of the parallelepiped associated to the lines is on the trisector line which is the line through $O$ and parallel to the interior trisector of the associated frame.*

*Conversely, if the direction of the lines are not in the special configuration, then the trisector contains a line if and only if it contains the center of the parallelepiped.*

**Proof.** With the parameters defined above, the coordinates of the center of the parallelepiped, easy to compute, are $X = (ax + \beta)/(2a), Y = (a\alpha + y)/2, Z = 0$. The equations of the trisector simplify easily to zero,

when substituting these coordinates and Equations (6) or (7) (in that order) in them. This proves that, if the trisector contains a line, the center of the parallelepiped lies on the bisector. As the set of triplets of lines whose trisector contains a line has at most four connected components (see Equations (6) and (7)), it suffices, by continuity, to choose a sample set of values for the parameters $a, \alpha, \beta$ to prove that the center of the parallelepiped is on the line. With $a = 3/2, \alpha = \beta = 2$ the computation is easy, since no square root appears.

We have already seen that the asymptotic directions of the trisector are the branches of the trisector of the edges of the parallelepiped supporting the basis vector of the associated frame. We have thus to prove that the direction of the line in the trisector is the interior trisector of the frame. If we circularly permute the lines, the origin of the frame is invariant and the basis vectors are permuted. Thus, the interior trisector is invariant while the other branches are permuted. As the line in the trisector of the skew lines is also invariant, its direction is necessarily that of the interior trisector.

To prove the converse, we substitute $X, Y, Z$ in the equations of the trisector by the coordinates of the center. The first equation becomes $(\beta + ax)(y + a\alpha) = 0$. Substituting $y$ by $-a\alpha$ (resp. $x$ by $-\beta/a$) in the second equation of the trisector, we get a polynomial which factors into $a^2\alpha^2 - \beta^2 - 1$ (resp. $a^2(1+\alpha^2) - \beta^2$) and a polynomial which, solved in $x$ (resp. $y$), gives Equation (6) (resp. Equation (7)). As the first factors are the equations of the special configurations, this finishes the proof. □

# F Maple-sheet computations

Computation of at least a point per connected component of $\mathcal{D}(\lambda, x, y, \alpha, \beta, a) < 0$

```
> vars:=[lambda,x,y,alpha,beta,a]:
> new_sa_component_hyp_neg(D,vars);

Pre-process..............
Computing critical values of a polynomial mapping from C^6 to C
Computing asymptotic critical values of a polynomial mapping from C^6 to C
"****************Enter in internal", [x, y,alpha, beta, a], [], [], [lambda]}
End of pre-process..............
Computing sampling points in a real hypersurface
Computing Critical Points using FGb (projection on lambda)
Computing Asymptotic Critical Values of u restricted to a hypersurface
Computing Critical Points using FGb (projection on x)
Computing Asymptotic Critical Values of x restricted to a hypersurface
Computing Critical Points using FGb (projection on y)
Computing Asymptotic Critical Values of y restricted to a hypersurface
Computing Critical Points using FGb (projection on alpha)
Computing Asymptotic Critical Values of alpha restricted to a hypersurface
Computing Critical Points using FGb (projection on beta)
Computing Asymptotic Critical Values of beta restricted to a hypersurface
Computing Critical Points using FGb (projection on a)
Computing Critical Points using FGb (projection on beta)
Computing Asymptotic Critical Values of beta restricted to a hypersurface
Computing Critical Points using FGb (projection on a)
Isolating real solutions of a zero-dimensional system using RS
Isolating real solutions of a zero-dimensional system using RS
Isolating real solutions of a zero-dimensional system using RS
Isolating real solutions of a zero-dimensional system using RS
Isolating real solutions of a zero-dimensional system using RS
Isolating real solutions of a zero-dimensional system using RS
Isolating real solutions of a zero-dimensional system using RS
Isolating real solutions of  a zero-dimensional system using RS
```

$$[]$$

Computation of at least a point per connected component of $\mathcal{D}(\lambda, x, y, \alpha, \beta, a) > 0$

```
> new_sa_component_hyp_neg(-D,vars);

[.........................]
```

$$\begin{aligned}
&[\{x=0,\lambda=0,a=-\tfrac{6752988915}{8589934592},\alpha=-1,y=0,\beta=0\},\\
&\{x=0,\lambda=0,a=\tfrac{6752988915}{8589934592},\alpha=-1,y=0,\beta=0\},\\
&\{x=0,\lambda=0,a=-\tfrac{6752988915}{8589934592},y=0,\beta=0,\alpha=1\},\\
&\{x=0,\lambda=0,a=\tfrac{6752988915}{8589934592},y=0,\beta=0,\alpha=1\},\\
&\{x=0,a=-\tfrac{6752988915}{8589934592},\lambda=2,\alpha=-1,y=0,\beta=0\},\\
&\{x=0,a=\tfrac{6752988915}{8589934592},\lambda=2,\alpha=-1,y=0,\beta=0\},\\
&\{x=0,a=-\tfrac{6752988915}{8589934592},\lambda=2,y=0,\beta=0,\alpha=1\},\\
&\{x=0,a=\tfrac{6752988915}{8589934592},\lambda=2,y=0,\beta=0,\alpha=1\}]
\end{aligned}$$

Table 1: For the proof of Lemma 3.

```
> Gamma:=(2*a*(y*alpha-x*beta)-(a^2-1))^2+3*(a*x+beta)^2+3*a^2*(y+a*alpha)^2+3*(a^2+1)^2;
```

$$\Gamma := (2a(\alpha y - \beta x) - a^2 + 1)^2 + 3(xa + \beta)^2 + 3a^2(y + a\alpha)^2 + 3(1 + a^2)^2$$

```
> [gros_fact, op(convert(grad(gros_fact,[a,x,y,alpha,beta]),list)),
> 1-u*(y+a*alpha), 1-v*(a*x+beta),1-w*(1+alpha^2+beta^2),1-t*Gamma)]:
> fgb_gbasis_elim(%,0,[u,v,w,t],[a,x,y,alpha,beta]);

pack_fgb_call_generic:   "FGb: 965.76 sec Maple: 975.98 sec"
```

[1]

Table 2: For the proof of the Main Lemma.

```
> sys:=subs(a=2,[gros_fact,op(convert(grad(gros_fact,[a,x,y,alpha,beta]),list))]):
> bs1:=factor(fgb_gbasis(sys,0,[x,y,alpha,beta],[])):  map(uu->op(0,uu),%), op(1,bs1[3]);
```

$$[+,+,*,+,+,+,+,+,+], \quad y+2\alpha$$

```
> [op(bs1),1-u*(y+2*alpha), 1-v*(2*x+beta),1-w*(1+alpha^2+beta^2)]:
> bs2:=factor(fgb_gbasis_elim(%,0,[u,v,w],[x,y,alpha,beta])):  map(uu->op(0,uu),%),map(degree,%);
```

$$[+,+,+,+],[6,6,6,6]$$

```
> bs3:=factor(fgb_gbasis_elim(bs2,0,[x],[y,alpha,beta])):map(uu->op(0,uu),%);
```

$$[^]$$

```
> bs4:=factor(fgb_gbasis([op(bs2),op(1,bs3[1])],0,[x,y,alpha,beta],[])):map(uu->op(0,uu),%);
```

$$[*,*,*,*,*,*,*,*,*,*,*,*,*,+,+,+,+]$$

```
> fgb_gbasis_elim([op(bs4),1-u*op(3,bs4[1])],0,[u],[x,y,alpha,beta]);
```

$$[1]$$

```
> bs5:=factor(fgb_gbasis([op(bs4),op(3,bs4[1])],0,[x,y,alpha,beta],[])):map(uu->op(0,uu),%);
```

$$[+,+,+,+,+,*,+,+,+,+,+,+,*,+,+,*,*,*,*,*,*,*,*,+,+,+,+]$$

```
> fgb_gbasis_elim([op(bs5),1-u*op(3,bs5[6])],0,[u],[x,y,alpha,beta]);
```

$$[1]$$

```
> bs6:=factor(fgb_gbasis([op(bs5),op(3,bs5[6])],0,[x,y,alpha,beta],[])):map(uu->op(0,uu),%);
```

$$[+,+,+,+,+,+,+,+,+,+,+,+,+,+,+,+]$$

```
> bs7:=factor(fgb_gbasis_elim(bs6,0,[y],[x,alpha,beta])):map(uu->op(0,uu),%);
```

$$[*,*,*,*,*,*,*,*,*,*,*,*,*,*,*,*,*,*,*,*,*,*,*,*,*,*,*,^]$$

```
> bs8:=factor(fgb_gbasis([op(bs6),op(1,bs7[nops(bs7)])],0,[x,y,alpha,beta],[])):map(uu->op(0,uu),%);
```

$$[+,+,+,+,+,+,+,+,+,+,\cdots,+,+,+,+,+,+,+,+,+]$$

```
> bs9:=factor(fgb_gbasis_elim(bs8,0,[alpha],[x,y,beta])):map(uu->op(0,uu),%);
```

$$[*,*,*,*,*,*,*,*,*,*,\cdots,*,*,*,*,*,*,*,*,*,*]$$

```
> fgb_gbasis_elim([op(bs9),1-u*op(nops(bs9[1]),bs9[1])],0,[u],[x,y,alpha,beta]);
```

$$[1]$$

```
> bs10:=factor(fgb_gbasis([op(bs8),op(nops(bs9[1]),bs9[1])],0,[x,y,alpha,beta],[])):
> map(uu->op(0,uu),%),op(2,bs10[3]);
```

$$[+,+,*,+,+,+,+,+,+,*,+,+,+,+,+,\cdots,+,+,+,+,+], \quad y+2\alpha$$

```
> [op(bs10),1-u*(1+alpha^2+beta^2),1-v*(y+2*alpha), 1-w*(2*x+beta)]:
> bs11:=factor(fgb_gbasis_elim(%,0,[u,v,w],[x,y,alpha,beta])):map(uu->op(0,uu),%);
```

$$[+,+,+,*,+,+,+,+,+,+,+,+,+,+,+,+]$$

```
> fgb_gbasis_elim([op(bs11),1-u*op(2,bs11[4])],0,[u],[x,y,alpha,beta]);
```

$$[1]$$

```
> bs12:=factor(fgb_gbasis([op(bs11),op(2,bs11[4])],0,[x,y,alpha,beta],[])):map(uu->op(0,uu),%),map(degree,%);
```

$$[+,+,+],[4,4,4]$$

```
> bs12[3];
> Gamma2:=(4*y*alpha-4*x*beta-3)^2+3*(2*x+beta)^2+12*(y+2*alpha)^2+75;
> simplify(Gamma2-bs12[3]);
```

$$16\alpha^2y^2+84-32\beta x\alpha y+16\beta^2x^2+12x^2+12y^2+24y\alpha+48\alpha^2+36\beta x+3\beta^2$$

$$\Gamma 2 := (4y\alpha-4\beta x-3)^2+3(2x+\beta)^2+12(y+2\alpha)^2+75$$

$$0$$

```
> [op(sys),1-u*(1+alpha^2+beta^2),1-v*(y+2*alpha),1-w*(2*x+beta),1-t*Gamma2]
> fgb_gbasis(%,0,[u,v,w,t],[x,y,alpha,beta]);
```

$$[1]$$

Table 3: About the proof of the Main Lemma.

```
> st := time():
> bs3:=factor(fgb_gbasis(bs2,0,[x],[y,alpha,beta])):
> map(degree,%,x);
> map(uu->op(0,uu),%%);
> nops(bs3);
```

$$[4, 3, 3, 3, 3, 2, 2, 2, 2, 2, 2, 2, 2, 2, 2, 2, 2, 2, 2, 2, 2, 2, 2, 2, 2, 2, 2, 2, 2, 2, 2, 2, 2, 1, 1, 1

```
> factor(subs(y=-a*alpha,big_fact));
```

$$(\alpha^4 a^4+2\beta x\alpha^2 a^3+x^2a^2+\beta^2x^2a^2-2a^2\alpha^2+1+\beta^2)$$
$$(\beta^2-4a^2-4a^2\alpha^2-4a^4-4a^4\alpha^2-2a\beta x-4\beta xa^3+x^2a^2)^2$$

```
> f0:=collect(op(1,%),x);  f1:=collect(op(1,op(2,%%)),x);
```

$$f0 := (a^2\beta^2+a^2)x^2+2\beta x\alpha^2a^3+\alpha^4a^4+1+\beta^2-2a^2\alpha^2$$
$$f1 := x^2a^2+(-2a\beta-4\beta a^3)x+\beta^2-4a^2-4a^2\alpha^2-4a^4-4a^4\alpha^2$$

```
> factor(subs(x=-beta/a,big_fact));
```

$$(\beta^4-2a^2\beta^2+a^4+a^4\alpha^2+2\beta^2\alpha ay+\alpha^2y^2a^2+y^2a^2)$$
$$(4+4\beta^2+4a^2+4a^2\beta^2-a^4\alpha^2+4ay\alpha+2ya^3\alpha-y^2a^2)^2$$

```
> g0:=collect(op(1,%),y);g1:=collect(op(1,op(2,%%)),y);
```

$$g0 := (a^2\alpha^2+a^2)y^2+2\beta^2\alpha ay+\beta^4-2a^2\beta^2+a^4+a^4\alpha^2$$
$$g1 := -y^2a^2+(4a\alpha+2a^3\alpha)y+4+4\beta^2+4a^2+4a^2\beta^2-a^4\alpha^2$$

Solutions of f1=0 in x and of g1=0 in y:

```
> map(uu->factor(uu),[solve(f1,x)]);
```

$$[\frac{2a^2\beta+\beta+2\sqrt{a^2(a^2+1)(\beta^2+1+\alpha^2)}}{a}, \frac{2a^2\beta+\beta-2\sqrt{a^2(a^2+1)(\beta^2+1+\alpha^2)}}{a}]$$

```
> map(uu->factor(uu),[solve(g1,y)]);
```

$$[\frac{\alpha a^2+2\alpha+2\sqrt{(a^2+1)(\beta^2+1+\alpha^2)}}{a}, \frac{\alpha a^2+2\alpha-2\sqrt{(a^2+1)(\beta^2+1+\alpha^2)}}{a}]$$

f0 is a sum of square:

```
> (a^2*alpha^2-1+a*beta*x)^2+(a*x+beta)^2;
> simplify(f0-%);
```

$$(a^2\alpha^2-1+a\beta x)^2+(xa+\beta)^2$$
$$0$$

a*x+beta and g1 are in the ideal generated by y+a*alpha, x*a+beta, and a^2*alpha^2-1+a*beta*x:

```
> gbasis([y+a*alpha,x*a+beta,a^2*alpha^2-1+a*beta*x],DRL([a,x,y,alpha,beta])):
> normalf(a*x+beta,%), normalf(g1,%);
```

$$0, 0$$

g0 is a sum of square:

```
> (a*y*alpha+beta^2-a^2)^2+a^2*(y+a*alpha)^2;
> simplify(g0-%);
```

$$(ay\alpha+\beta^2-a^2)^2+a^2(y+a\alpha)^2$$
$$0$$

y+a*alpha and f1 are in the ideal generated by x*a+beta, y+a*alpha, and a^2*alpha^2-1+a*beta*x:

```
> gbasis([x*a+beta,y+a*alpha,a*y*alpha+beta^2-a^2],DRL([a,x,y,alpha,beta])):
> normalf(y+a*alpha,%), normalf(f1,%);
```

$$0, 0$$

Table 5: For the proof of Lemma 7.

```
> comp1 := [y = -a*alpha, x =
> (2*beta*a^2+beta)/a+2*sqrt((beta^2+1+alpha^2)*(1+a^2))];
```

$$comp1 := [y = -\alpha a, x = \frac{2\beta a^2+\beta}{a} + 2\sqrt{(1+\alpha^2+\beta^2)(1+a^2)}]$$

We prove that the characteristic equation has no real root on this component.

```
> factor(subs(comp1,Char_eq));
> irrat:=op(2,%):
```

$$a^2(4-4\beta^2\lambda^3+8a^2-4\lambda^3+\lambda^4-8\lambda-16\alpha^2\lambda a^2-8\beta^2\lambda a^2+8\alpha^2+4\beta^2+12a^2\alpha^2+12a^2\beta^2+4a^4+8a^4\beta^2+4a^4\alpha^2-8\lambda a^2-16\alpha^2\lambda$$
$$-8\beta^2\lambda+8\lambda^2+4\lambda^2a^2+8a^2\alpha^2\lambda^2+4\beta^2\lambda^2a^2+8\beta^2\lambda^2-8\beta\alpha a^3\lambda-8\beta\alpha\lambda a+8\beta\alpha a^3+8a\beta\alpha+8\alpha\sqrt{\%1}-8\lambda a^2\alpha\sqrt{\%1}+\lambda^4\beta^2$$
$$+\lambda^4\alpha^2+4\lambda^2\beta\sqrt{\%1}a-8\lambda\beta\sqrt{\%1}a+12\alpha^2\lambda^2-4\alpha^2\lambda^3+8\beta\sqrt{\%1}a+8a^2\alpha\sqrt{\%1}+8\beta a^3\sqrt{\%1}-4\lambda^3\alpha\sqrt{\%1}+12\lambda^2\alpha\sqrt{\%1}-16\lambda\alpha\sqrt{\%1})$$
$$\%1 := (\beta^2+1+\alpha^2)(1+a^2)$$

Consider the product of the characteristic polynomial with its algebraic conjugate:

```
> T:=expand(irrat*subs(sqrt((1+a^2)*(alpha^2+beta^2+1))=-sqrt((1+a^2)*(alpha^2
> +beta^2+1)),irrat)):
```

The real semi-algebraic set defined by T-1/2<0 is empty:

```
> new_sa_component_hyp_neg(T-1/2,[a,alpha,beta,lambda]);
```

```
Pre-process..............
Computing critical values of a polynomial mapping from C^4 to C
Computing asymptotic critical values of a polynomial mapping from C^4 to C
"**********************Enter in internal", [alpha,beta, lambda], [], [], [a]
End of pre-process..............
Computing sampling points in a real hypersurface
Computing Critical Points using FGb (projection on a)
Computing Asymptotic Critical Values of a restricted to a hypersurface
Computing Critical Points using FGb (projection on alpha)
Computing Asymptotic Critical Values of alpha restricted to a hypersurface
Computing Asymptotic Critical Values of alpha restricted to a hypersurface
Computing Critical Points using FGb (projection on beta)
Computing Asymptotic Critical Values of beta restricted to a hypersurface
Computing Critical Points using FGb (projection on lambda)
Isolating real solutions of a zero-dimensional system using RS
Isolating real solutions of a zero-dimensional system using RS
Isolating real solutions of a zero-dimensional system using RS
Isolating real solutions of a zero-dimensional system using RS
```

$$[]$$

Consider all the 3x3 minors of the matrix $P(\lambda)$ of the pencil:

```
> ldet:=NULL:
> for i to 4 do for j from i to 4 do
> ldet:=ldet,det(minor(P,i,j)):
> od od:
```

The rank of $P(\lambda)$ is always 3 or 4 since there is no common zeros of the minors:

```
> [ldet,1-t*(1+alpha^2+beta^2)*(1+a^2)*(-beta+y+a*x-a*alpha)*(-beta-y+a*x+a*alpha)]:
> fgb_gbasis_elim(%,0,[],[t,a,x,y,alpha,beta,lambda]);
```

$$[1]$$

Table 6: For the proof of Lemma 8.